

Study of Far Infrared Cavity in Interstellar Medium Located Nearby White Dwarf and Galactic Infrared Loop

B. B. Sapkota^{1*}, B. Aryal²

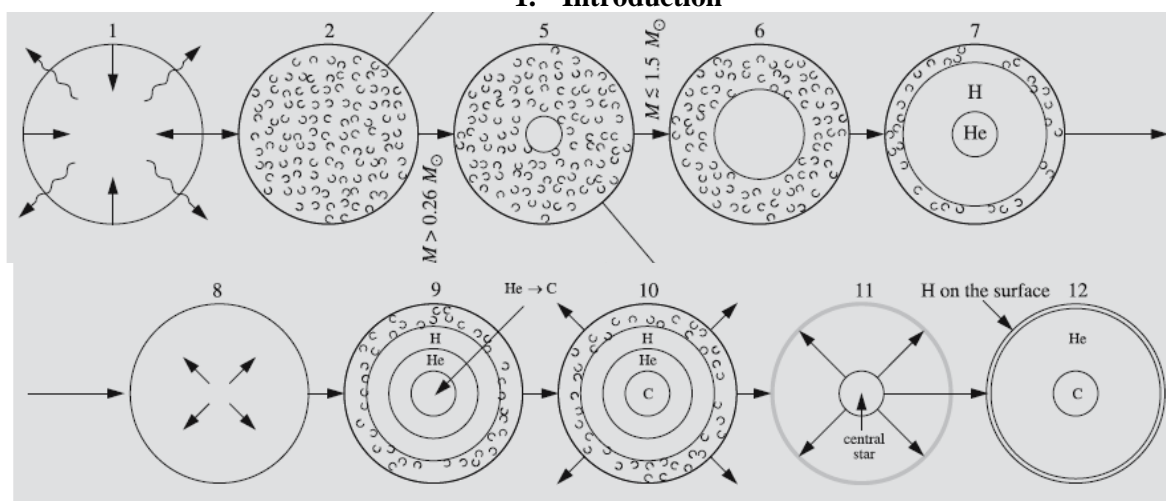
¹Mahendra Ratna Campus, Tahachal, Tribhuvan University, Kathmandu, Nepal

²Central Department of Physics, Tribhuvan University, Kirtipur, Nepal

Abstract: We study the variation of dust colour temperature, mass of cavities located nearby white dwarf WD0531-022 and Galactic Infrared Loop G206-17. It is found that the temperatures of this cavity varies 25.15K to 25.66K. The dust colour temperature contour map, mass contour map, flux density contour map, visual extinction contour map, the flux density at 60 μ m versus 100 μ m plot, Gaussian plot of dust colour temperature and Gaussian plot of mass nearby white dwarf is discussed.

Keywords: White dwarf, Galactic Infrared Loop, Contour map, Cavity, Flux density, Visual extinction.

1. Introduction



The evolution of star is shown in figure. Though, the star has different phase of evolution and different sizes, the radius is drawn to be same. First, the gas cloud is contracting rapidly in free fall (step 1). The radiation escapes easily from cloud due to low density. When density of gas increases, radiation transfer becomes difficult and tends to warm up the gas. The gas contracts until completely ionised, and star is called protostar and is in hydrostatic equilibrium (step 2). When the mass of star is less than $0.26M_{\text{sun}}$ and state is in main sequence star, no stable white dwarf is formed (so steps 3 and 4 is not shown figure).

When temperature of star is more than 4×10^6 K and mass is greater than $0.26M_{\text{sun}}$ and less than $1.5M_{\text{sun}}$ (step 5) the center of star is in radiative (step 6). In this phase the hydrogen in the core changes to helium by proton proton chain. At the end of main sequence, the helium is in the core and hydrogen in the shell (step 7). The outer part expands and giant phase starts. The contracting helium is in degenerate form and temperature rises to 10^8 K. By triple alpha process, the helium in the core changes to carbon continuously (step 8, 9, and 10). The outer parts expands and star loses some its mass. The expanding envelope forms planetary nebula (step 11) and core becomes white dwarf (step 12) [1].

2. Literature Review

Collimated jets are observed in a variety of astrophysical objects. They have been noticed in quasars, active galactic nuclei, stellar binaries, young stellar objects, planetary nebulae (PNe) and pulsars. However, despite large efforts, there is still no definite concurrence as to the mechanisms that give rise to the acceleration and to collimation of these jets. Herbig-Haro (HH) jets (Bally & Reipurth 2002) and jets in PNe (Sahai 2002) are among the best studied classes and there is growing evidence that both probably not only share morphological similarities, but also the same basic physical principles [2,3]. R. Weinberger and B. Armsdorfer (2004) detected these adjacent objects while systematically searching for large dust structures around PNe and

white dwarfs on IRAS 12-100 μm maps (via sky view virtual observatory) [4]. The objects - which morphological closely resemble HH jets - are visible at 60 and 100 μm only. Although the IRAS mission took place two decades ago, the maps are still not exhausted of their riches, as they could demonstrate by e. g. the discovery jet like structures (size $\sim 9^\circ$ each) found in the far infrared.

B. Aryal and R. Weinberger (2006) presented a large new high galactic latitude cone like far infrared nebula (RA=08^h 27^m 5^s, Dec=+25^o 53' 59" (J2000)) at 100 μm and 60 μm IRAS images. With SIMBAD they found three possible candidates, namely an M-type emission star (RX J082605.8+262740) carbon white dwarf star (WD 0824+288) and pulsar (PSR B0823+26). These were selected because (1) all of them are rather nearby, (2) they might emit a wind in the course of evolution (3) they show some peculiar properties, and (4) They are placed at a suitable apparent location with respect to the nebula [5].

Kiss et al. presented the results of an investigation of the large scale structure of the diffuse interstellar medium in the 2nd Galactic Quadrant. 145 loops were identified on IRAS based far infrared maps. Their catalogue lists their basic physical properties. The distribution clearly suggests that there is an efficient process that can generate loop like features at high galactic latitudes. Distances are provided for 30 loops [6]. Konyves et al. identified 462 far infrared loops analysed their individual FIR properties (including large scale structure) and their distribution. They formed the catalogue of FIR loops in the Galaxy [7]. Jha et al. studied dust colour temperature and dust mass of four far infrared loops. They selected the candidate by assuming the distance between pulsar and loop is less than 1⁰. They had taken low latitude loops and believed to be formed due to high pressure events occurred in the past (e.g. supernova explosion). They found out that the dust colour temperature and dust mass distribution maps satisfy Cosmological principle (i.e. low temperature region has greater density) [8].

3. Materials and Methods

We have taken a database of 1978 number of white dwarfs which are listed in the catalogue of Holberg et al. [9]. Out of which we have selected WD0531-022. For distance of white dwarf we taken reference from far infrared loops studied by Konyves et al. [7]. The name of loop is G206-17. The major and minor diameter of loop is 1.4⁰ (or 7.4 pc) and 0.9⁰ (or 4.8 pc) respectively. We have carried out a systematic search of IRAS maps available in the sky view virtual observatory (<http://skyview.gsfc.nasa.gov>). The sample white dwarf has the right ascension of 05^h 34^m 20^s and declination of -02^o 14^m 32^s in equatorial coordinate system. Again the Galactic infrared loop G206-17 has the right ascension of 05^h 36^m 53.7^s and declination of -02^o 30^m 07^s in the same coordinate. The following input parameters were used for the search: (1) Coordinate: J2000, (2) Projection: Gnomonic (Tan), (3) Image size (pixel): 500 \times 500 (4) Image size (degrees): 0.5⁰ \times 0.5⁰ and 2⁰ \times 2⁰ (5) Brightness Scaling: Histogram Equalization (HistEq) (6) Colour Table: Stern Special.

We have downloaded Flexible Image Transport System (FITS) v3 image of the selected region. We have taken FITS format of 0.5⁰ \times 0.5⁰ at 60 and 100 μm for the image processing. Using ALADIN v2.5 software, the FITS image carries the information concerning the position, flux density, temperature, mass, and visual extinction for each pixel. It is an interactive sky atlas developed and maintained by the Center de Données astronomiques de Strasbourg (CDS) for the identification of astronomical sources through visual analysis.

In order to separate the region of minimum flux density region, contours are drawn at 60 and 100 μm respectively. Because we are interested to study temperature, mass and visual extinction of the region. We intend to study the cavity like structure at 60 μm and 100 μm . The flux density of each pixel in the region of interest is noted.

Dust Colour Estimation:

Dust color temperature can be estimated by using following relation [10]

$$T_d = -96 \frac{1}{\ln\{R \times 0.6^{(3+\beta)}\}} \dots \dots (3.1)$$

where R is given by

$$R = \frac{F(60 \mu\text{m})}{F(100 \mu\text{m})} \dots \dots (3.2)$$

F(60 μm) and F(100 μm) are the flux densities at 60 μm and 100 μm , respectively.

Here we use $\beta=2$ for cloud of shape crystalline, dielectric or metals [11].

Mass Estimation:

The mass of the dust can be determined by the following relation [12]

$$M_{dust} = \frac{4 a \rho}{3 Q_v} \left[\frac{S_v D^2}{B(v, T)} \right] \dots \dots \dots (3.3)$$

Where a , ρ , Q_v , and s_v represent weighted grain size, grain density, grain emissivity and flux density of the region of interest, respectively. Here,

$$S_v = f \times 5.288 \times 10^{-9} \text{ MJy/Sr}$$

The distance (D) to the cavity is 305 pc, known from [7].

The Planck's function is given by[13],

$$B(\nu, T) = \frac{2h\nu^3}{c^2} \left[\frac{1}{e^{h\nu/kT} - 1} \right] \dots \dots (3.4)$$

Where h , c , ν , and T represent Planck's constant, velocity, frequency of light, and average temperature of region respectively.

By using, $a=0.1 \mu\text{m}$, $\rho=3000 \text{ kgm}^{-3}$, and $Q_v=0.0010$ for $100 \mu\text{m}$ and 0.0046 for $60 \mu\text{m}$ respectively, the expressions (3.3) and (3.4) takes the form [14]:

$$M_{\text{dust}}=0.4 \left[\frac{S_v D^2}{B(\nu, T)} \right] \dots \dots \dots (3.5)$$

We use the equation (3.5) for the calculation of the dust mass

Visual Extinction Estimation:

It is the reduction in brightness or amount of light or other radiation from celestial body or star as a result of absorption or scattering of radiation by interstellar dust. The visual extinction A_v relates distance and magnitude by the relation [1]

$$m - M = 5 \log r - 5 + A_v \dots \dots \dots (3.6)$$

Where m and M represent the apparent and absolute magnitudes respectively[15].

$$A_v (\text{mag}) = 15.078[1 - \exp\{-\tau(100)/641.3\}] \dots \dots \dots (3.7)$$

Where,

$$\tau(100) = \frac{F(100 \mu\text{m})}{B(\nu, T)} = \text{Optical depth} \dots \dots \dots (3.8)$$

$F(100 \mu\text{m})$ =Flux density at $100 \mu\text{m}$ and $B(\nu, T)$ is planck's function

4. Result and Discussion

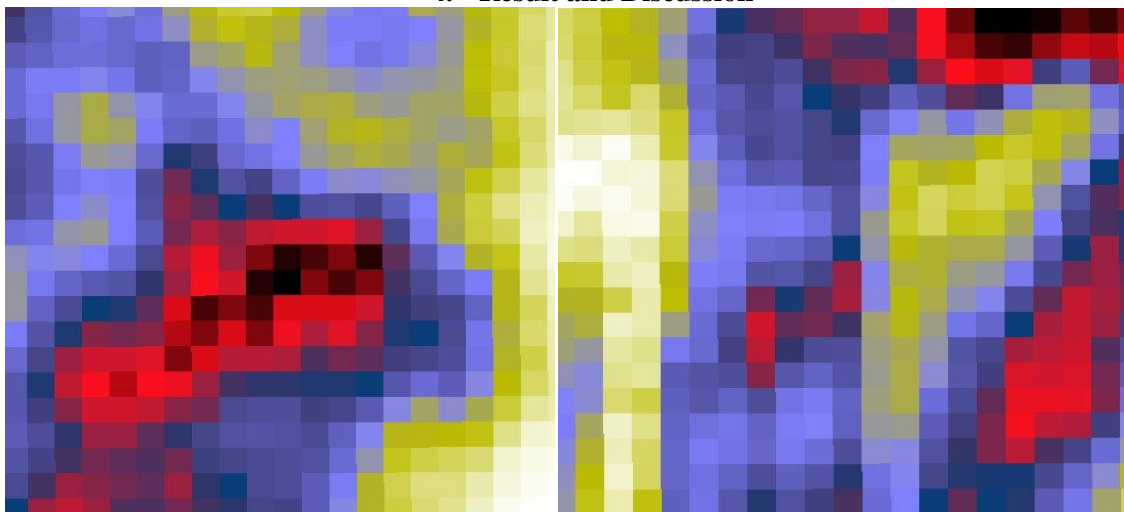


Figure 4. 1: $0.5^0 \times 0.5^0$ JPEG image of the region centered at R.A.(J2000)= $05^h 34^m 20^s$, Dec. (J2000)= $-02^0 14^m 32^s$ of WD 0531-022 (left) and centered at R.A.(J2000)= $05^h 36^m 53^s$, Dec. (J2000)= $-02^0 30^m 07^s$ of G206-17 (right)

Figure 4.1 represents the JPEG image of white dwarf WD0531-022 and Galactic infrared loop G206-17. In both figure black colour represents the region of minimum flux and white colour represents maximum flux.

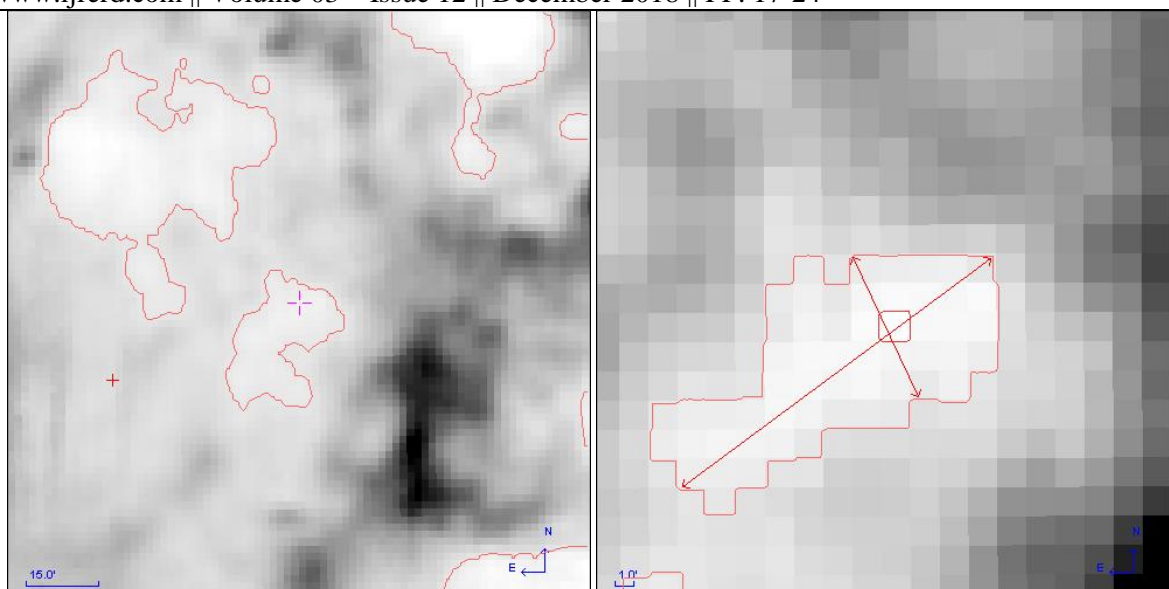


Figure 4. $2.2^0 \times 2^0$ FITS image of the region centered at R.A.(J2000)= $05^h 34^m 20^s$, Dec. (J2000)= $-02^{\circ} 14^m 32^s$ of WD 0531-022 and at R.A.(J2000)= $05^h 36^m 53^s$, Dec. (J2000)= $-02^{\circ} 30^m 07^s$ of G206-17 in south east of WD (left). Cavity formed by taking $0.5^0 \times 0.5^0$ FITS image of the region centered at R.A.(J2000)= $05^h 34^m 20^s$, Dec. (J2000)= $-02^{\circ} 14^m 32^s$ of WD 0531-022 (right).The minor and major diameters passing through minimum flux are also shown.The isocontour level is 25. The distance between WD0531-022 and G206-17 is 0.7^0 (or 3.7 pc).

Figure (4.2) represents cavity formed located nearby WD0531-022 (right).The size of cavity is ($20.07 \times 7.8'$) (or 1.9 pc \times 0.7 pc).The major diameter of G206-17 is 7.4 pc is greater than major diameter of WD0531-022.So the WD0531-022 lies inside the loop G206-17.

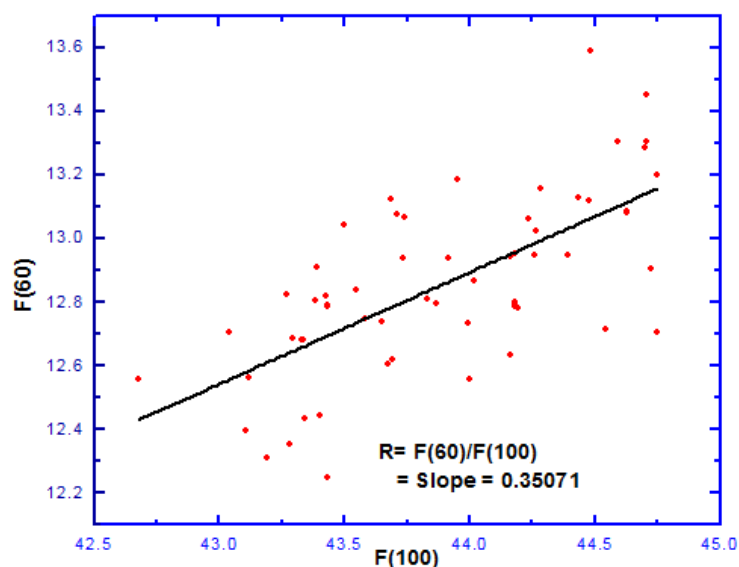


Figure 4.3: F (60 micron) versus F(100 micron) in white dwarfs WD0531-022

Figure (4.3) represents the relative flux density of concerned white dwarf. The linear curve has slope(R)= 0.35 and correlation coefficient is 0.43.Due to low slope the average temperature is 26.64K where as individual

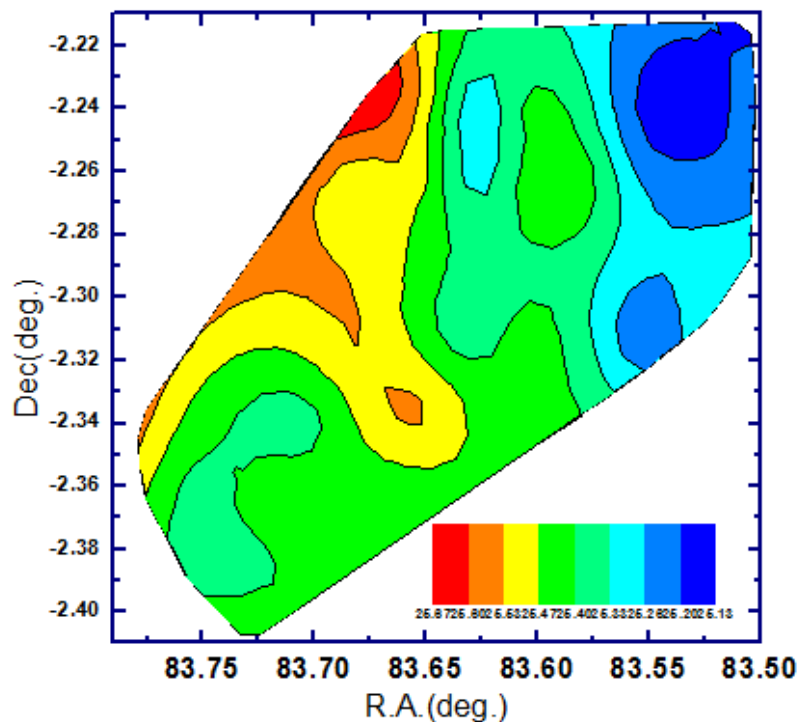


Figure 4.4: Contour map of dust colour temperature of white dwarfs WD0531-022

Figure (4.4) represents dust colour temperature with respect to right ascension (R.A.) and declination (dec.) The blue colour is the minimum temperature is north direction and red colour is at north east direction has maximum temperature.

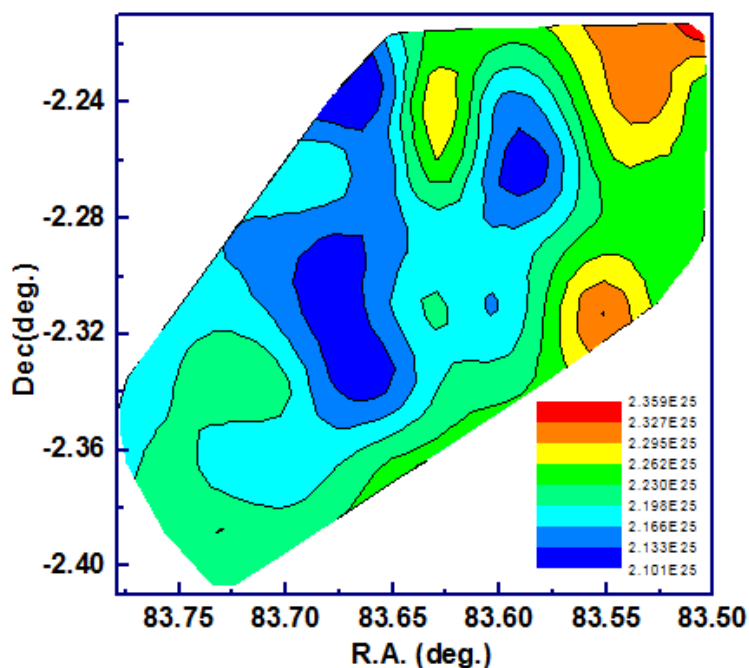


Figure 4.5: Contour map of mass distribution of white dwarf WD0531-022

Figure (4.5) also represents two dimensional contour plot with projection of mass in XY plane. The central region of the cavity is covered by minimum mass (ie blue color).The maximum mass (ie red colour) in the cavity is in the north south direction .From contour map of mass and temperature distribution it is found that ,the cavities follow cosmological principle.It means the distribution is homogenous and isotropic.

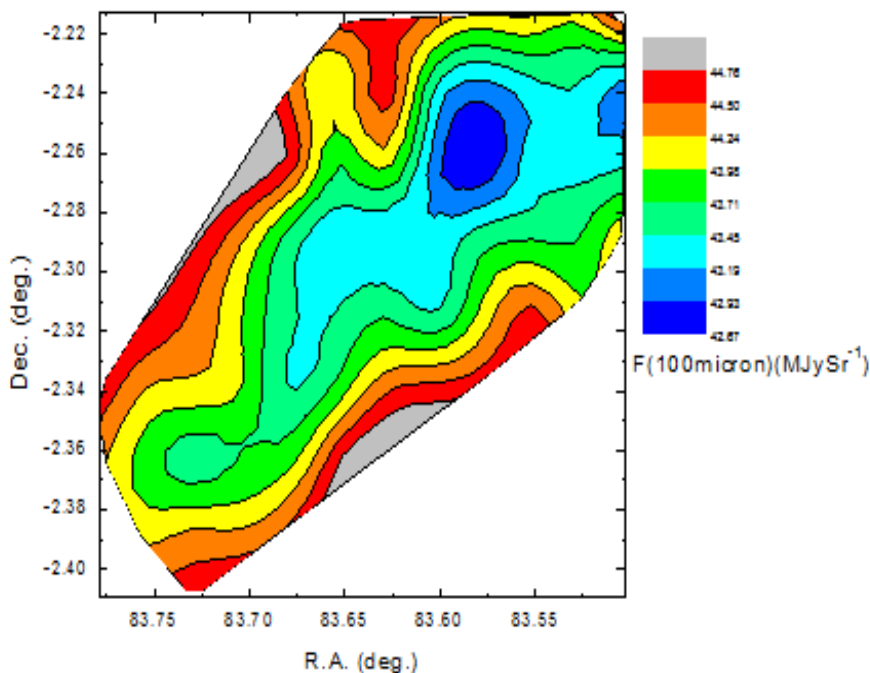


Figure 4.6: Contour map of flux distribution of white dwarf WD0531-022

Figure (4.6) also represents two dimensional contour plot with projection of flux in XY plane. The central region of the cavity is covered by minimum mass (ie blue color).The maximum mass (ie silver colour) in the cavity is in the north east and south west direction .

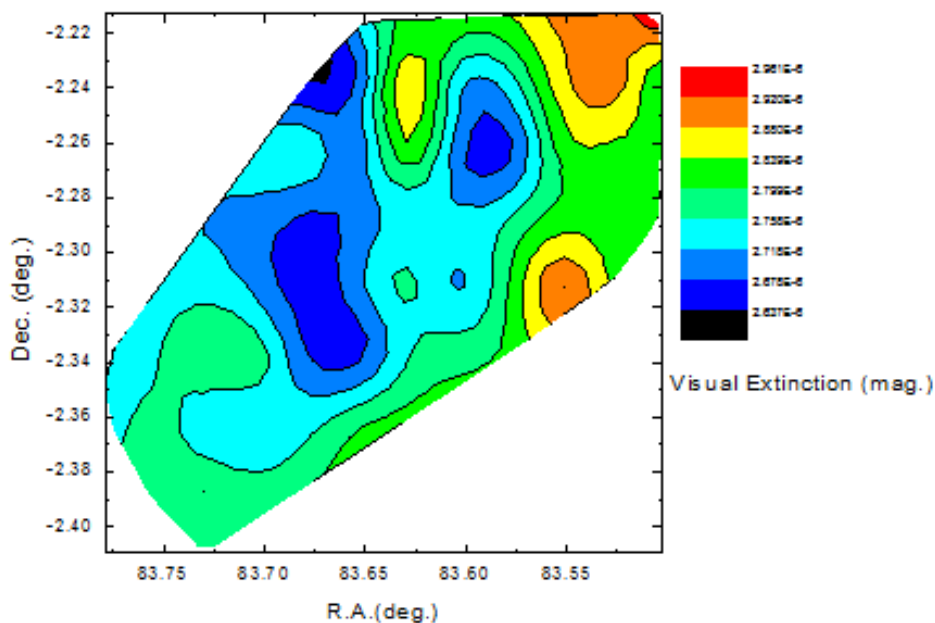


Figure 4.7: Contour map of visual extinction distribution of white dwarf WD0531-022

Figure (4.7) also represents two dimensional contour plot with projection of visual extinction in XY plane. The north east to central position of the cavity is covered by minimum mass (ie black and blue color).The maximum visual extinction (ie red colour) in the cavity is in the north direction .By comparing contour map of visual extinction and temperature we get higher the visual extinction ,lower the temperature.

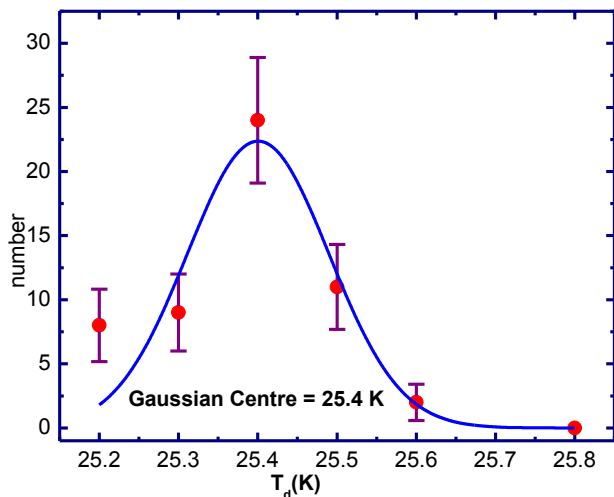


Figure 4.8: Distribution of dust colour temperature of white dwarfs WD0531-022 .The blue solid curve represents the Gaussian fit .The $\pm 1\sigma$ is statistical error bars (i.e .red) and $\sigma=\sqrt{n}$.

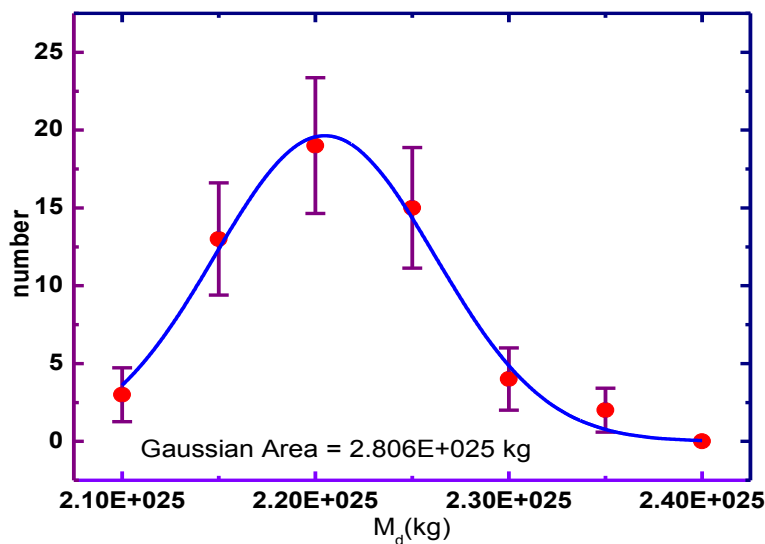


Figure 4.9: Distribution of dust mass of white dwarfs WD0531-022. The blue solid curve represents the Gaussian fit .The $\pm 1\sigma$ is statistical error bars (i.e .red) and $\sigma=\sqrt{n}$.

Figure (4.8) indicates that the distribution is nearly Gaussian and is positive skewness (i.e.skew to the right) .The cavity formed around the white dwarf WD0531-022 is in nearly thermal equilibrium and is stable. Similarly , figure (4.9) indicates that the mass distribution shows same nature as temperature distribution. The Gaussian area is greater in mass than the temperature distribution.

5. Conclusion

The average temperature of the cavity formed by dust located nearby WD0531-022 is found to be 26.64K . The temperature of dust inside the cavity varies from 25.15K to 25.66K. There is less difference between maximum and minimum temperature suggests that the dust in the cavity is in thermal equilibrium and core of cavity is stable. The total mass of dust is 1.24×10^{27} kg (i.e. $6.4 \times 10^{-4} M_{\odot}$). Contour map of mass and temperature distribution indicates that the cavities follow cosmological principle. It means the distribution is homogenous and isotropic. The size of cavity formed by nearby white dwarf WD0531-022 is $1.9 \text{ pc} \times 0.7 \text{ pc}$. The small shift from Gaussian nature in dust colour temperature and mass distribution indicates that the cavity is formed by external sources e.g. nearby other white dwarfs and supernova explosion.

References

- [1]. Karttunen, H., Kroeoger, P., Oja, H., Poutanen, M. & Donner, K.J. (2007). *Fundamental of Astronomy*. Springer Berlin Heidelberg, Fifth Edition. USA.
- [2]. Bally, J., B. & Reipurth, B. (2002). Recent Development in the Study of Herbig-Haro Objects. *RMxAA*, (13)1-7.
- [3]. Sahai, R. & Brilliant, S. (2002). Proper Motion in the Knotty Bipolar Jet in Henize 2-90. *The Astrophysical Journal*, L123-L127.
- [4]. Weinberger, R. & Armsdorfer, B. (2004). A Pair of 9° Long Dust Jets Ejected From Evolved Stars. *ASPCS*, (313), L16-L19.
- [5]. Aryal, B. & Weinberger, R. (2006). A new large high latitude cone like far-IR nebula". *Astronomy & Astrophysics*, (448), 213-219.
- [6]. Kiss, Cs., Moor, A. & Toth, L.V. (2004). Far Infrared Loops in the 2nd Galactic Quadrant". *Astronomy & Astrophysics*, (418), 131-141.
- [7]. Konyves, V., Kiss, Cs., Moor, A., Kiss, Z. & Toth, L. V. (2007). Catalogue of Far infrared Loops in the Galaxy. *Astronomy & Astrophysics*, (463), 3, 1227.
- [8]. Jha, A. K., Aryal, B. & Weinberger, R. (2017). A Study of Dust Colour Temperature and Dust Mass Distribution Of Far Infrared Loops. *RMxAA*, (53), 467-476.
- [9]. Holberg, J.B., Oswalt, Terry D. & Sion, E. M. (2002). A Determination of the Local density of White Dwarf Stars. *The Astrophysical Journal*, (571), L512-L518.
- [10]. Schnee, L.S., Ridge, N.A., Goodman, A. A & Jason, G.L. (2005). A Complete Look at the Use of IRAS Emission Maps to Estimate Extinction and Dust Temperature. *Astrophysical Journal*. (634), L442-L450.
- [11]. Dupac, X., Bernard J.P., Boudet, N., Giard, M., Lamarre, J.M., Meny, C. Pajot, F. Ristorcelli, I, Serra, G., Stepnik, B. & Torre, J.P. (2003). Inverse Temperature Dependent of the Dust Submillimeter Spectral Index. *Astronomy & Astrophysics*, (404), L11-L15.
- [12]. Hildebrand, R. H. (1983). The Determination of Cloud Masses and Dust Characteristics from Sub millimeter Thermal Emission. *Q. Journal of Royal Astronomical Society* (24), 267-282
- [13]. Beichman, C. A., Neugebauer, G., Habing, H. J., Clegg, P. E., Chester, T. J. (1988). *Infrared Astronomical Satellite (IRAS) Catalogues and Atlases I: Explanatory Supplement*. US Government Printing Office, Washington.
- [14]. Young, K., Philips, T.G., & Knapp, G.R. (1993). Circumstellar Shells resolved in IRAS Survey data II-Analysis. *Astrophysical Journal*, (409), 725
- [15]. Wood, D. O. S., Myres, P. C., & Daugherty, D.A. (1994). IRAS Images of Nearby Dark Clouds. *The Astrophysical Journal Supplement*, (95), 457-501.